Retinal Vessel Segmentation

Dr. Debdoot Sheet
Assistant Professor, Department of Electrical Engineering
Principal Investigator, Kharagpur Learning, Imaging and Visualization Group
Indian Institute of Technology Kharagpur

www.facweb.iitkgp.ernet.in/~debdoot/

Contents

- Motivation
- Datasets
- Prior Art
- Recent Contributions
  - Learning of statistical mechanics
  - Autoencoder based approach
  - Domain adaptation
- Endnote

Motivation

- Fundus imaging is used for screening of
  - Diabetic retinopathy
  - Glaucoma
  - Age-related macular degeneration
  - Hypertension and Stroke induced changes
- Challenges include
  - Vessels, fovea, optic disc – localization and segmentation
  - Pathology detection
  - Image quality assessment

Datasets

Image Sciences Institute

ABOUT PEOPLE RESEARCH EDUCATION VACANCIES

Publications / Theses Library / Gallery / Databases / Software / Spin-offs

DRIVE: Results Browser

Next Prev Go to 4 Magnification factor: 0.2 display soft classifcation when available

Display the following: input gold standard human observer Chaudhuri Jiang Niemeijer Perez Staal Zana

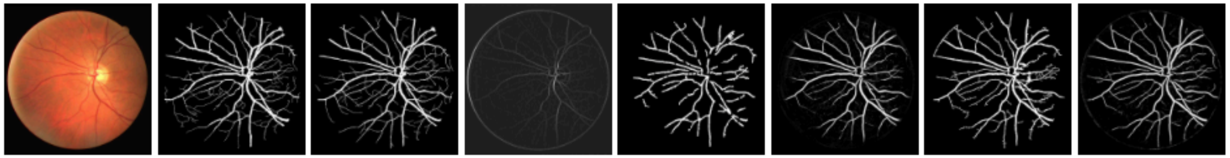

Results for case 4.

Displayed	Sensitivity	Specificity	Accuracy	Az
1. Input				
2. Gold standard				
3. Human observer	0.783	0.974	0.949	
4. Chaudhuri	0.286	0.986	0.893	0.906
5. Jiang	0.631	0.970	0.924	
6. Niemeijer	0.717	0.983	0.948	0.938
7. Perez	0.776	0.948	0.925	
8. Staal	0.737	0.979	0.947	0.951

http://www.isi.uu.nl/Research/Databases/DRIVE/

Notes

1. The images displayed here are for viewing purposes only. Do not use these images and segmentations for experiments, as all images are compressed.

Contact Us | BIS | ImagO | Utrecht University | UMC Utrecht | ISI - Intranet

Datasets

http://cecas.clemson.edu/~ahoover/stare/

The data below is described in:

A. Hoover, V. Kouznetsova and M. Goldbaum, "Locating Blood Vessels in Retinal Images by Piece-wise Threhsold Probing of a Matched Filter Response", *IEEE Transactions on Medical Imaging* , vol. 19 no. 3, pp. 203-210, March 2000.

Twenty images used for experiments:

image 0001	image 0002	image 0003	image 0004	image 0005	image 0044	image 0077	image 0081

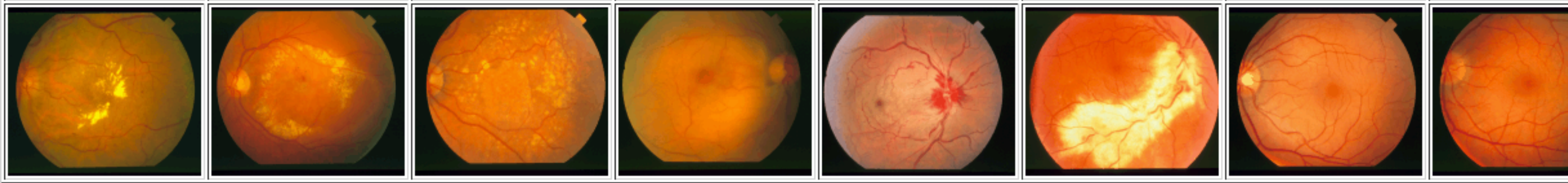

The twenty images are available packaged in a single archive file (tar format) containing compressed (using gnuzip) portable pixmap (PPM) format images.

Hand labeled vessel network provided by Adam Hoover

image 0001	image 0002	image 0003	image 0004	image 0005	image 0044	image 0077	image 0081

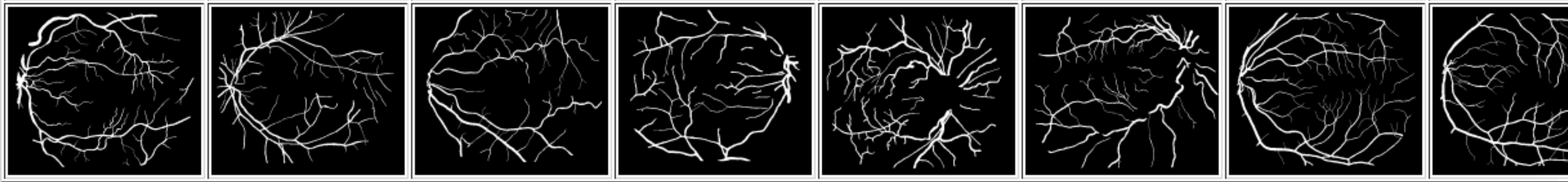

The hand labelings are available packaged in a single archive file (tar format) containing compressed (using gnuzip) portable pixmap (PPM) format images.

Datasets

- Standard Diabetic Retinopathy Dataset
  - http://www.it.lut.fi/project/imageret/diaretdb1/
- High Resolution Fundus Image Dataset
  - https://www5.cs.fau.de/research/data/fundus-images/
- CHASE
  - https://blogs.kingston.ac.uk/retinal/chasedb1/

Prior Art

- Vessel detection in white light Fundus imaging
  - Necessary for reporting of pathologies
  - Reduces clinician's dependency on FA
  - Solutions include
    - Staal et al. (2004)
    - Niemeijer et al. (2004)
    - Zana et al. (2001)
    - Jiang et al. (2003)
    - Martinez-Perez et al. (1999)
    - Chaudhuri et al. (1989)

- Limitations
  - Less Accurate (< 94%)
  - High inter-observer variability ($\kappa<0.71$)
  - Performance less than 2nd human-observer (Acc.=95%, $\kappa=0.76$)

RECENT CONTRIBUTIONS

Debdoot Sheet, Sri Phani Krishna Karri, Sailesh Conjeti, Sambuddha Ghosh, Jyotirmoy Chatterjee, Ajoy Kumar Ray, "Detection of retinal vessels in fundus images through transfer learning of tissue specific photon interaction statistical physics", Biomedical Imaging (ISBI), 2013 IEEE 10th International Symposium.

LEARNING OF STATISTICAL MECHANICS

Physics of Retinal Imaging

$$B(x,y,\lambda) = [R(x,y,\lambda)L(x,y,\lambda) * p(x,y,\lambda)]t(\lambda)$$

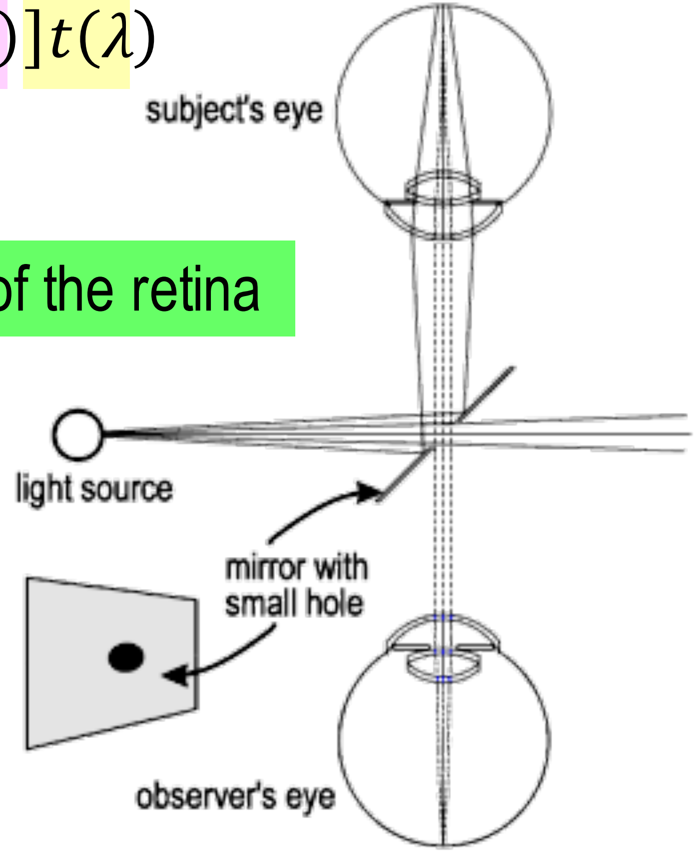

Spatially varying spectral reflectance pattern of the retina

Spatially varying illumination model

PSF of the ophthalmoscope

Spectral transmission of ophthalmoscope

Statistical Physics of Tissue-Photon Interaction

$$D = (K \quad T + N_{DC} + N_S + N_R)A + N_Q$$

Photo-current readout

External quantum efficiency of sensor

Rate of photon induced electron generation

Integration time

Amplification factor

Dark-current noise

Shot noise

Readout noise

Quantization noise

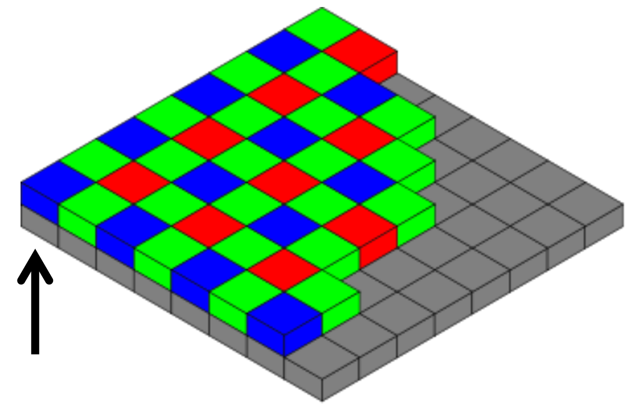

$$N_{DC}, N_S, N_R, N_Q << K \quad T$$

$$D \quad AK \quad T = \quad T$$

Statistical Physics of Tissue-Photon Interaction

$$f(d|\rho,T') \propto \frac{(\rho T')^d e^{-\rho T'}}{d!} \lambda \in [\lambda_1, \lambda_2]$$

$$T = E[d] = \mathrm{var}(d)$$

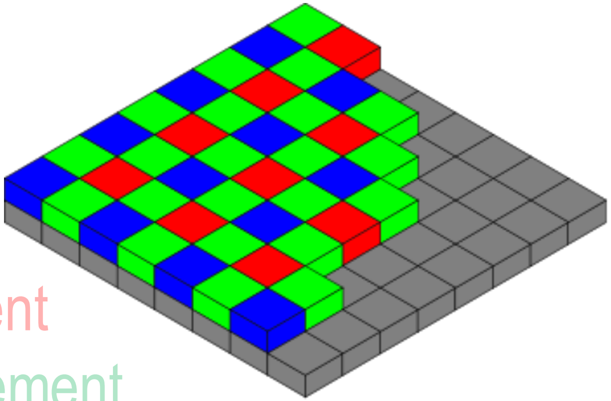

$f\left(d_R \mid {}_R, T\right)$ Distribution for RED sensor element

$f\left(d_G \mid {}_G, T\right)$ Distribution for GREEN sensor element

$f\left(d_B \mid {}_B, T\right)$ Distribution for BLUE sensor element

Multiscale photon density estimation

Vessel Detection Framework

Training Image

Learn TPI Model

$$H(\quad | \quad , I; \{I\}_{\text{train}})$$

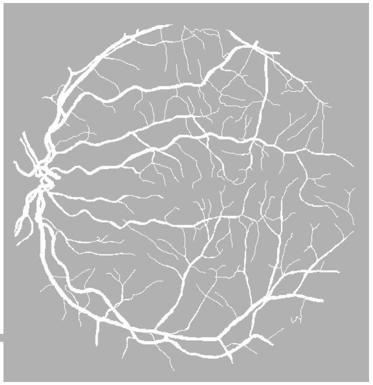

Ground Truth Labels

Test Image

Learn TPI Model

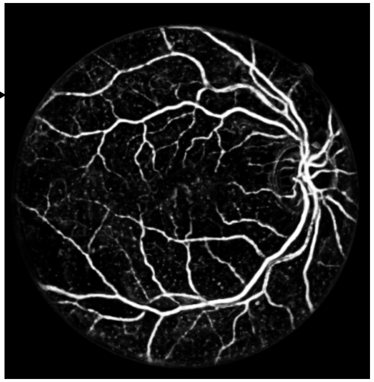

Vessel Detection Probab.

Performance Assessment

(a) Image (b) Ground truth (c) Proposed (d) 2nd Observer (e) Staal et al.

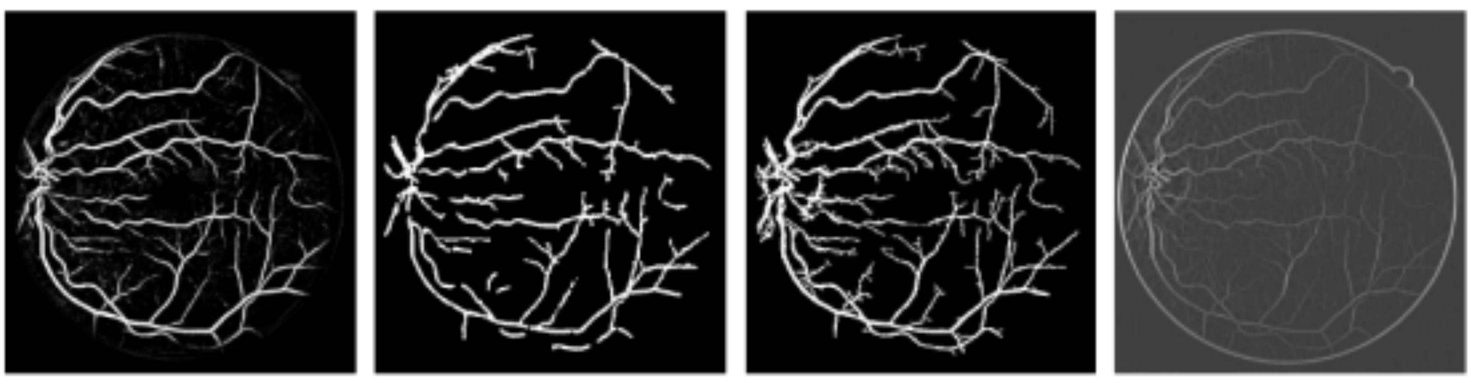

(f) Niemeijer et al. (g) Jiang et al. (h) Martínez-Pérez et al. (i) Chaudhuri et al.

Performance Assessment

	Max. avg. Accuracy	Kappa
Proposed method	**0.9766**	**0.8213**
Second observer	0.9473	0.7589
Staal et al [7].	0.9422	-
Niemeijer et al.	0.9416	0.7145
Zana et al.	0.9377	0.6971
Jiang et al.	0.9212	0.6399
Martínez-Pérez et al.	0.9181	0.6389
Chaudhuri et al.	0.8773	0.3357

Performance Assessment

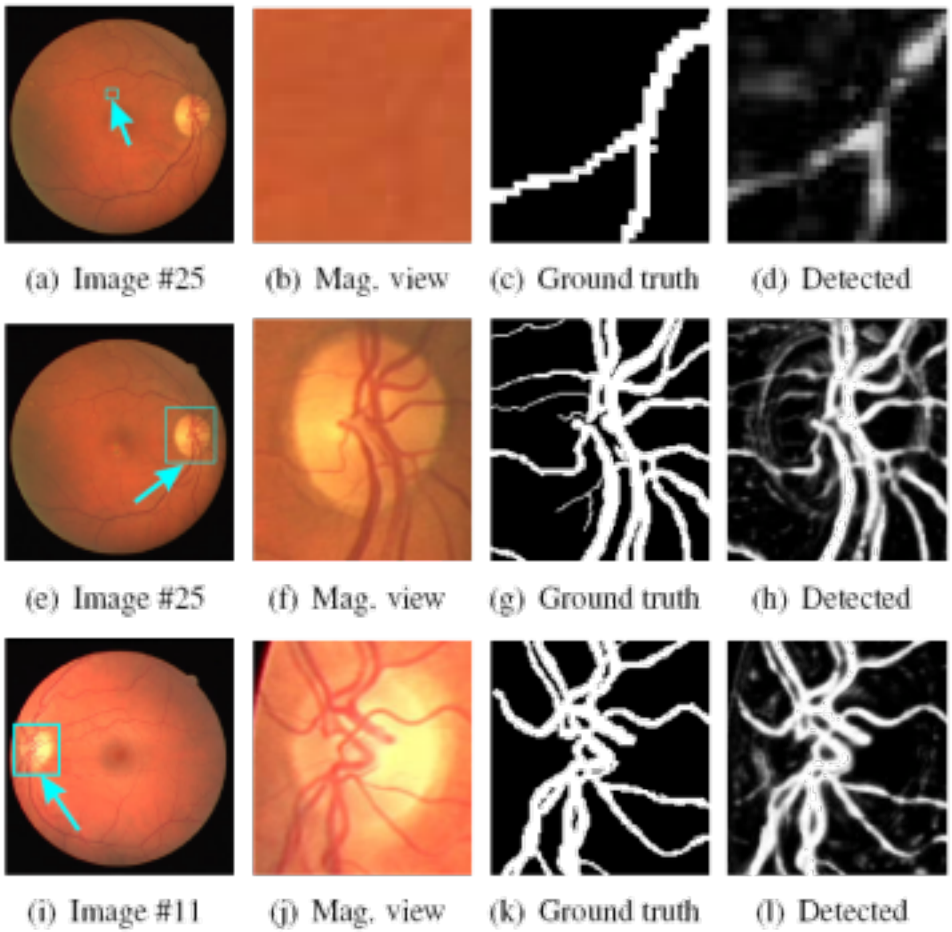

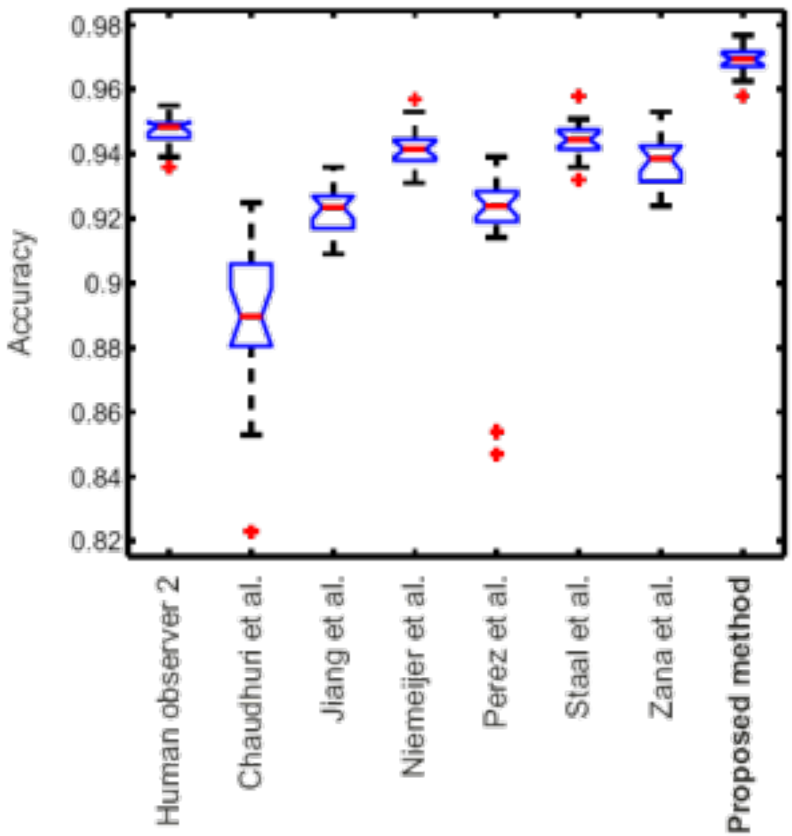

Maji D, Santara A, Ghosh S, Sheet D, Mitra P, "Deep Neural Network and Random Forest Hybrid Architecture for Learning to Detect Retinal Vessels in Fundus Images", in *Proc. EMBC* 2015.

AUTOENCODERS FOR RETINAL VESSEL SEGMENTATION

Heuristics in State of Art

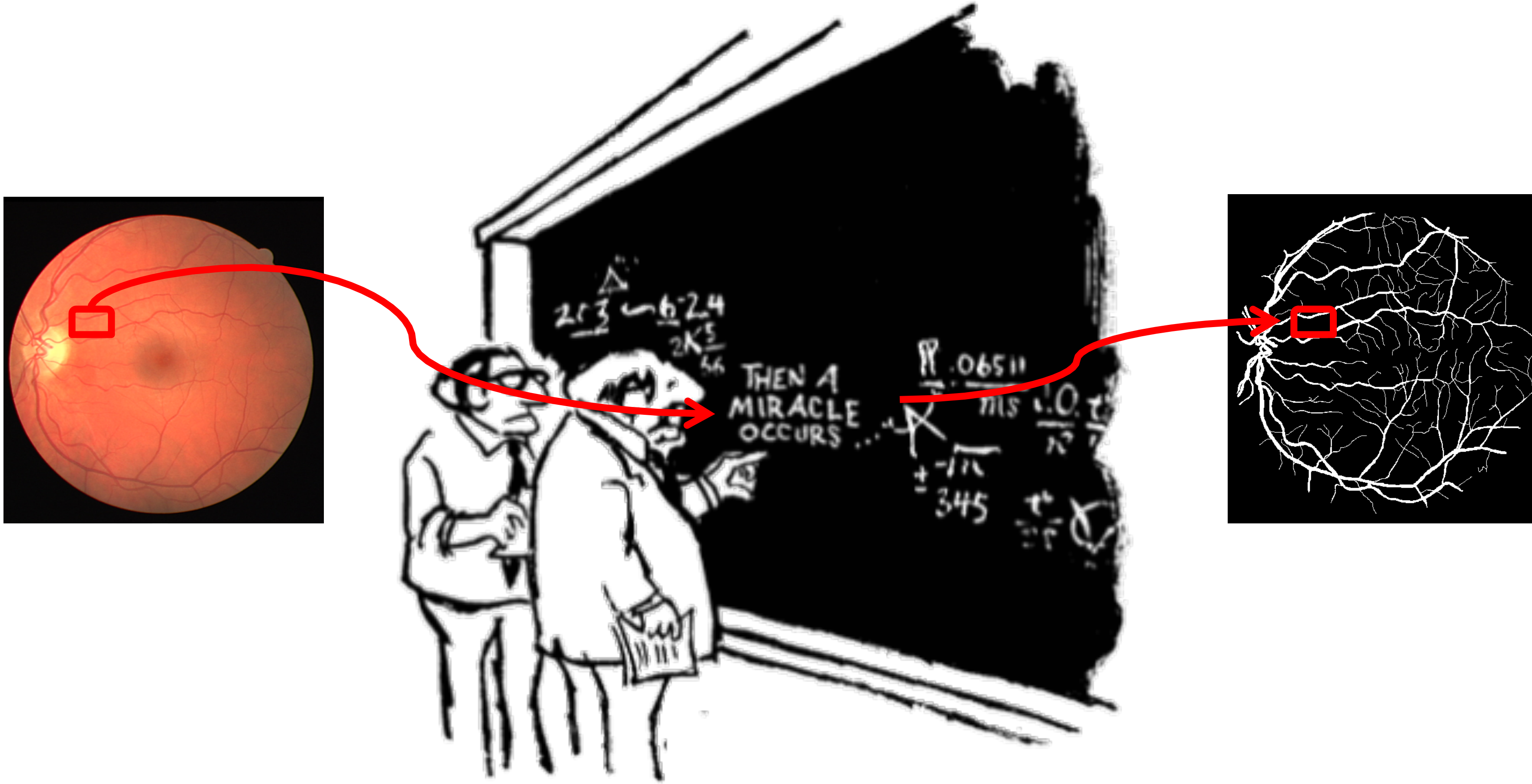

Using an Autoencoder

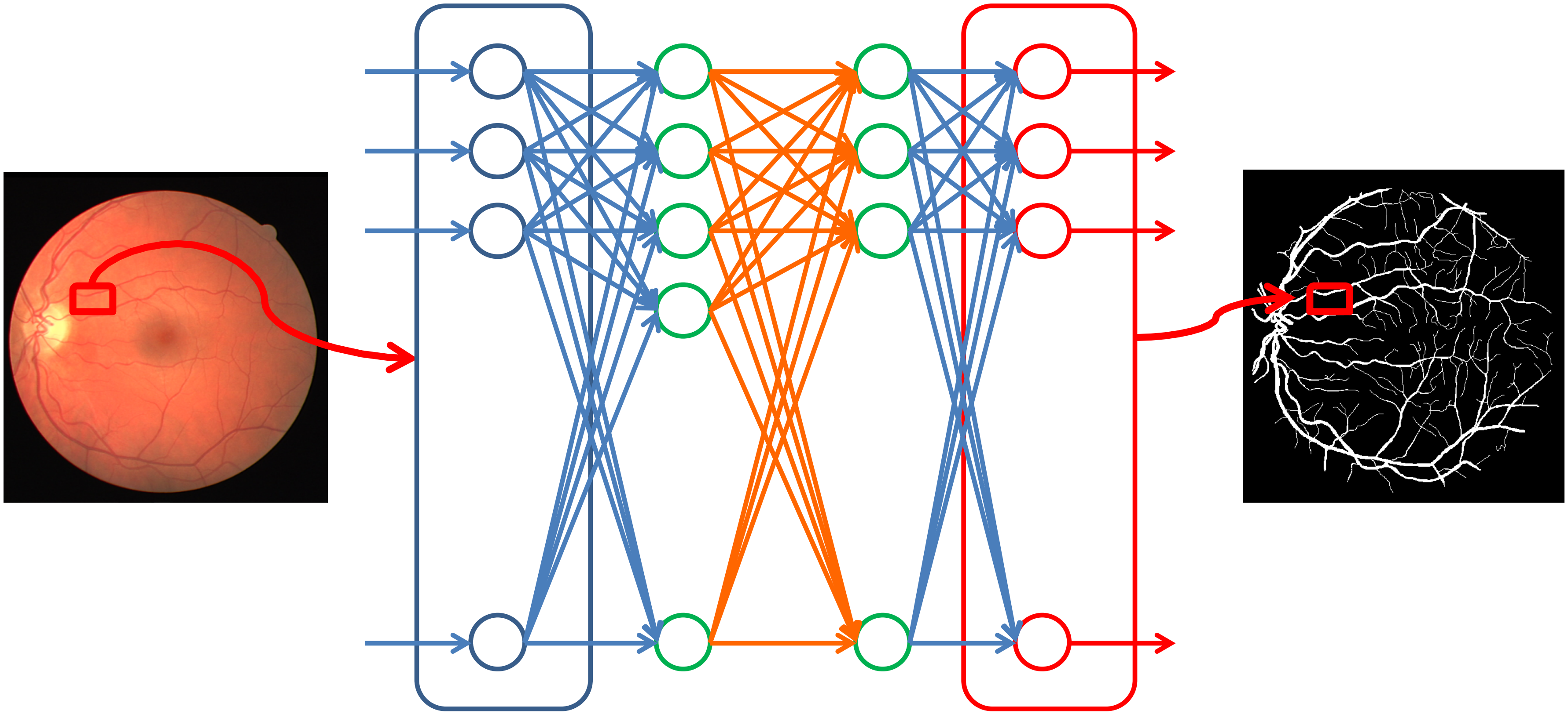

Learnt Manifestations

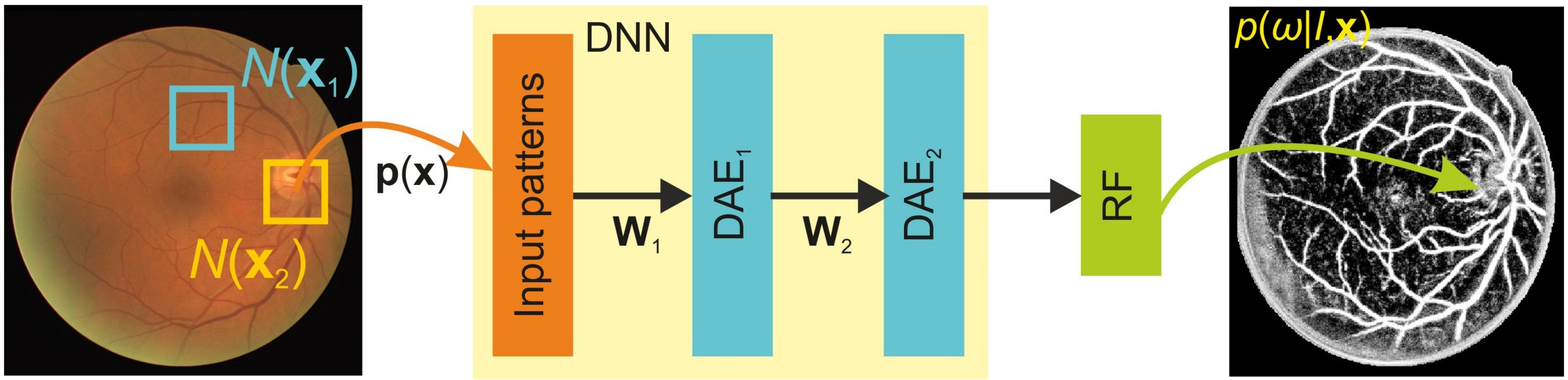

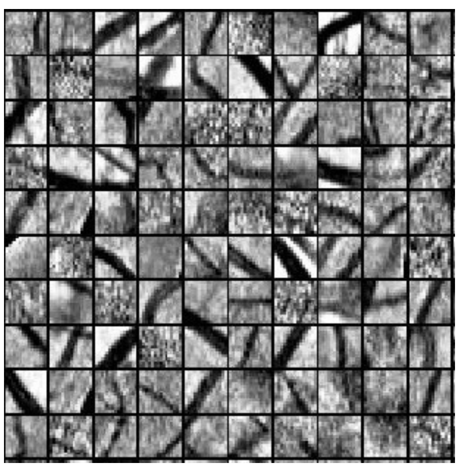

Sample patches

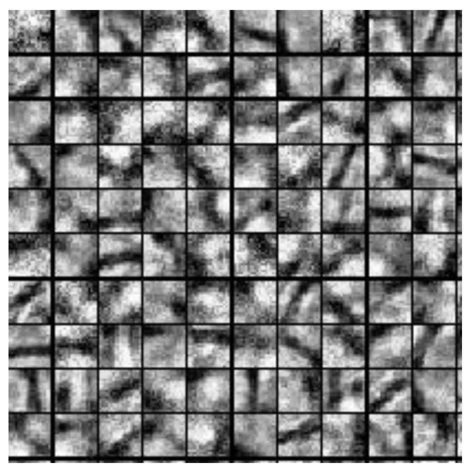

Weights of layer 1

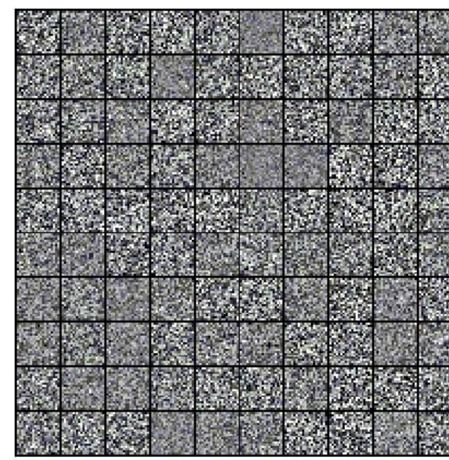

Weights of layer 2

Results

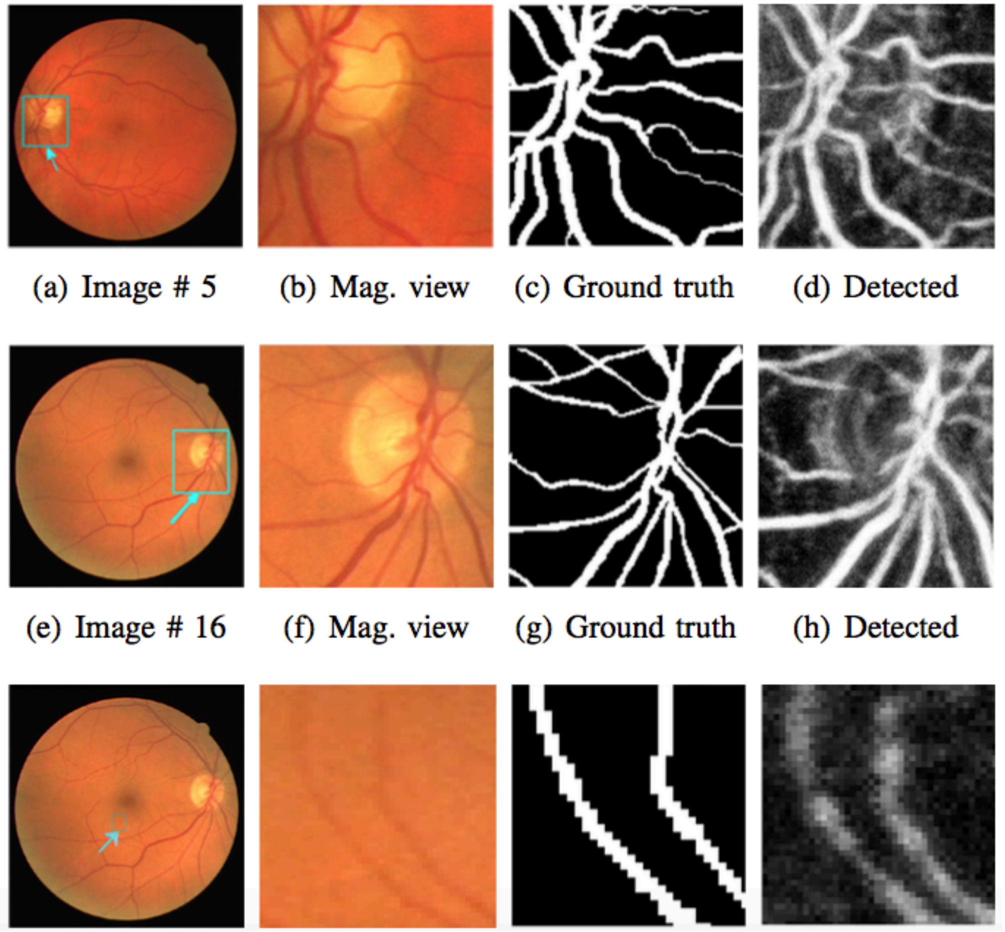
(a) Image # 5 (b) Mag. view (c) Ground truth (d) Detected

(e) Image # 16 (f) Mag. view (g) Ground truth (h) Detected

A. Guha Roy and D. Sheet, “Domain Adaptation in Stacked Autoencoders using Systematic Dropout”, in *Proc. Asian Conf. Patt. Recognition*, 2015.

DOMAIN ADAPTATION FOR VESSEL SEGMENTATION

Domain Adaptation

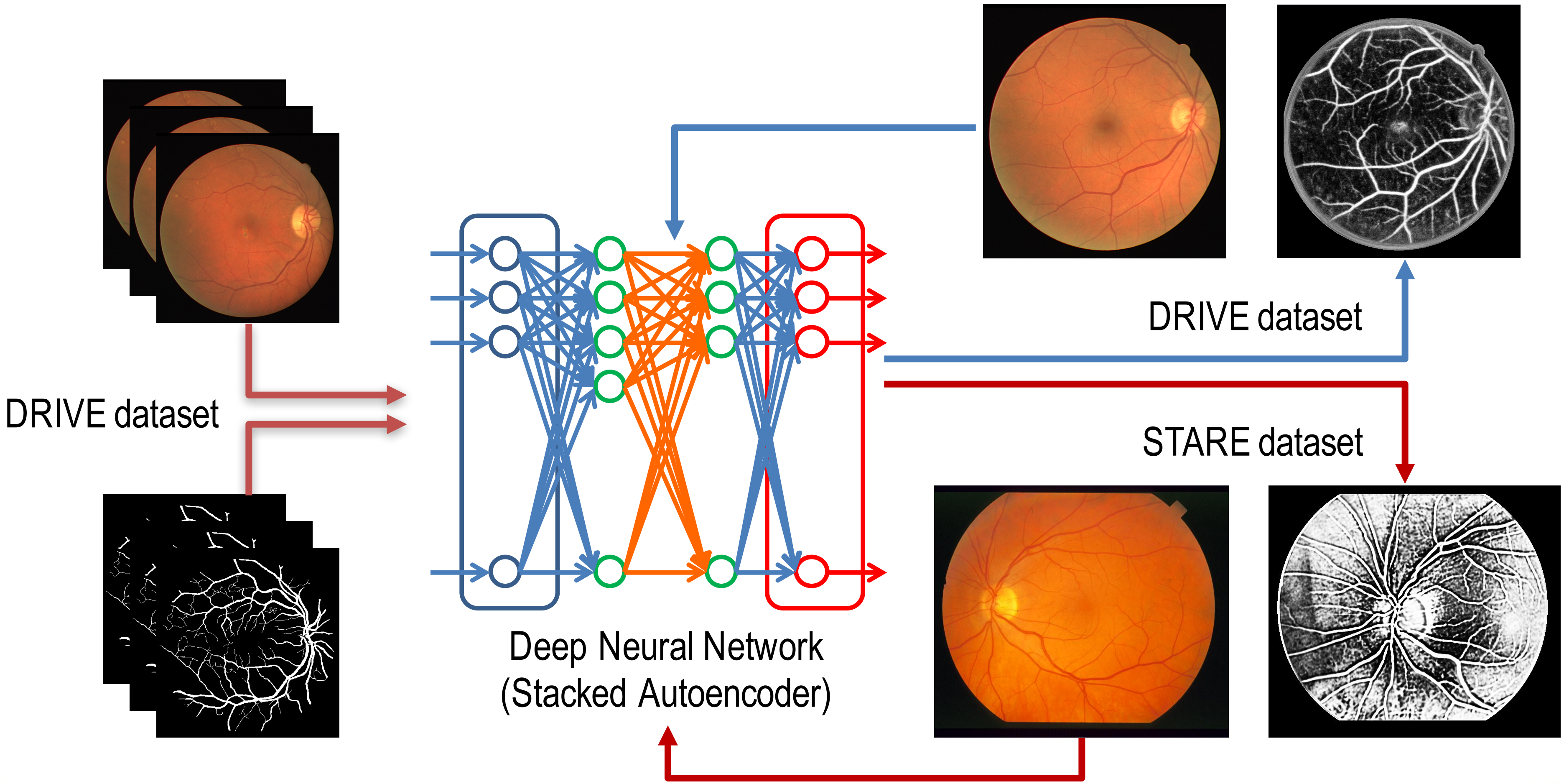

Demystifying

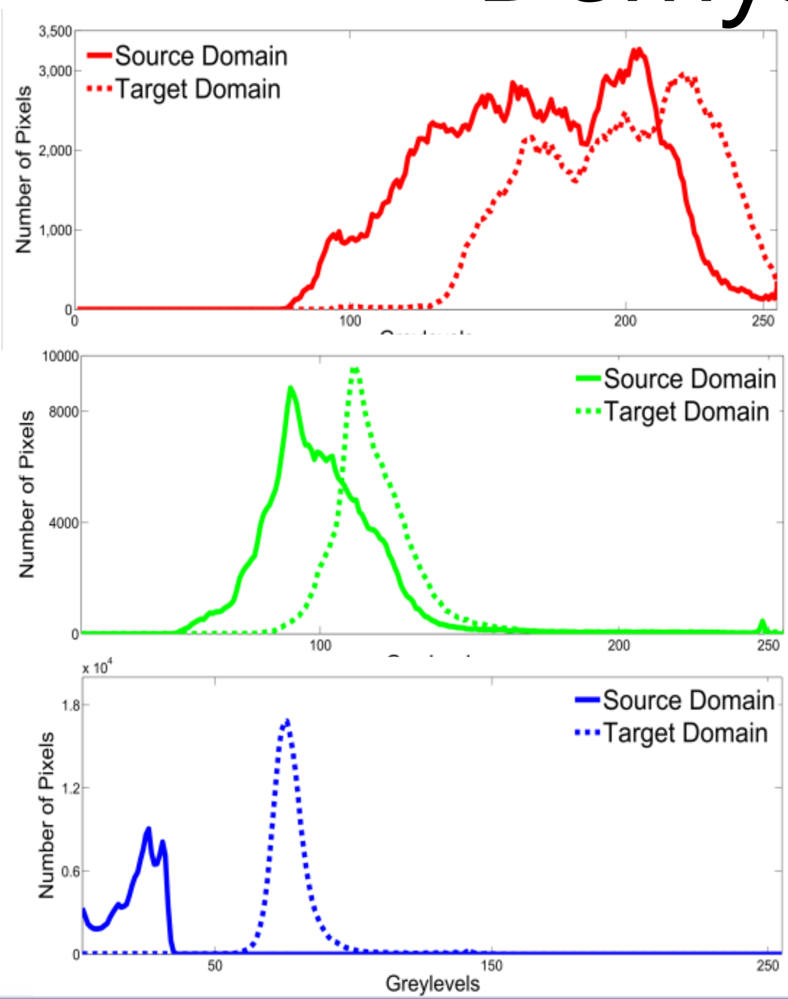

DRIVE dataset

STARE dataset

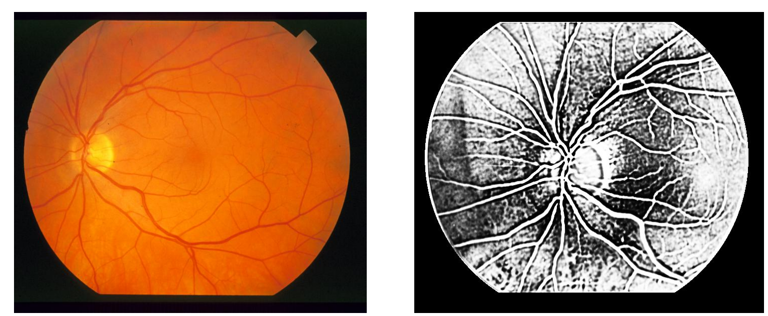

Definitions

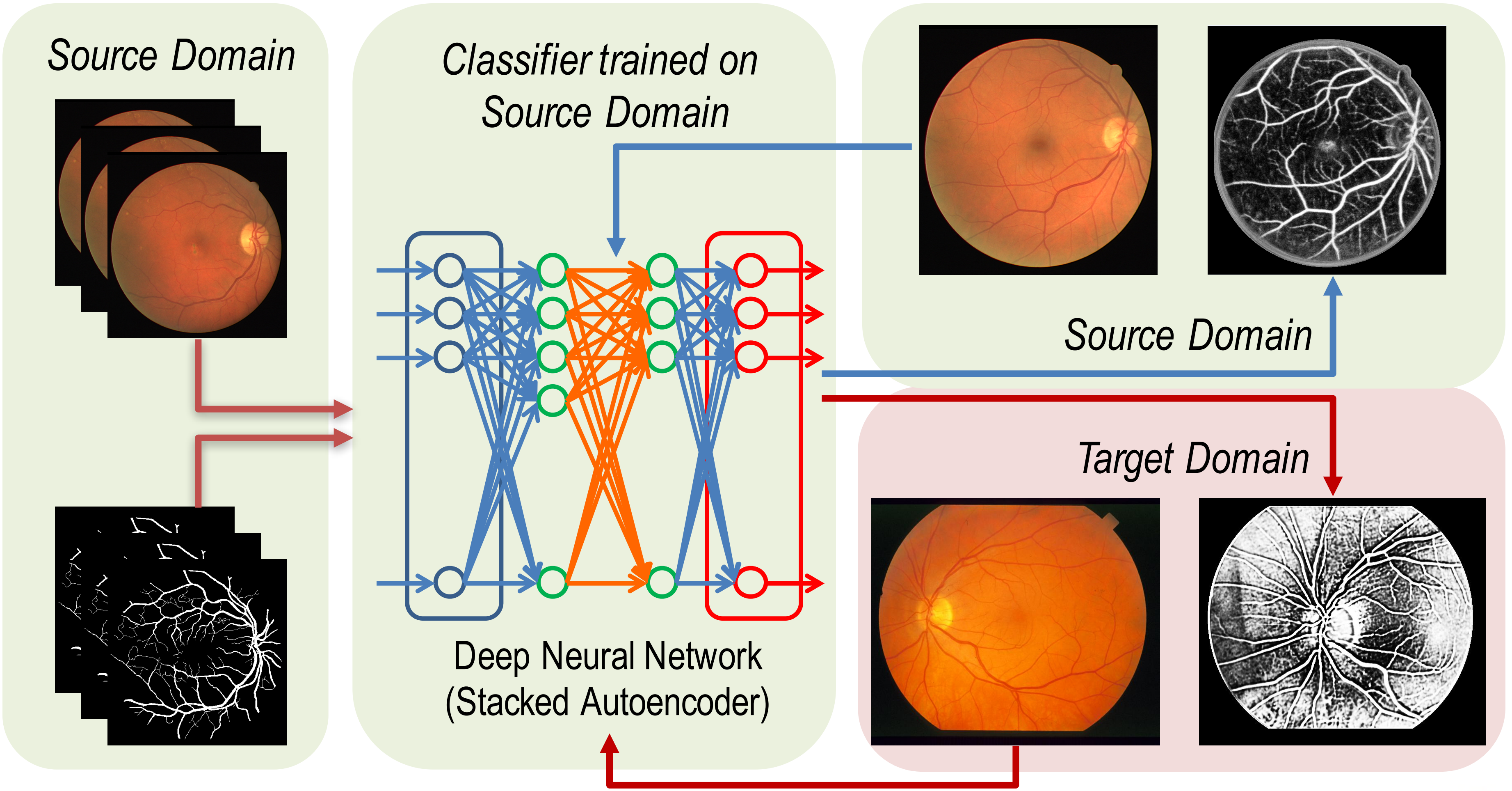

Definitions

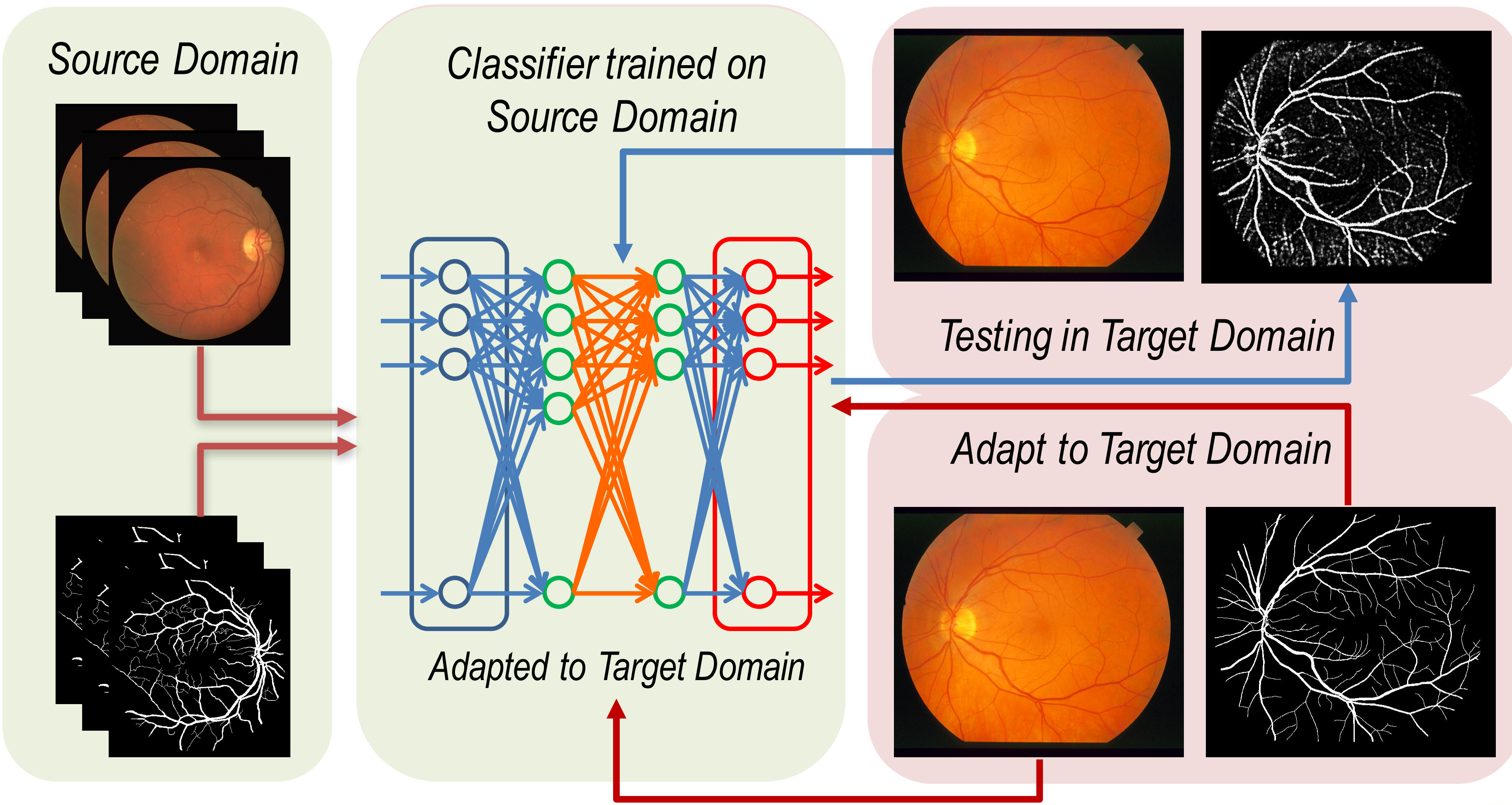

Origin and Notations

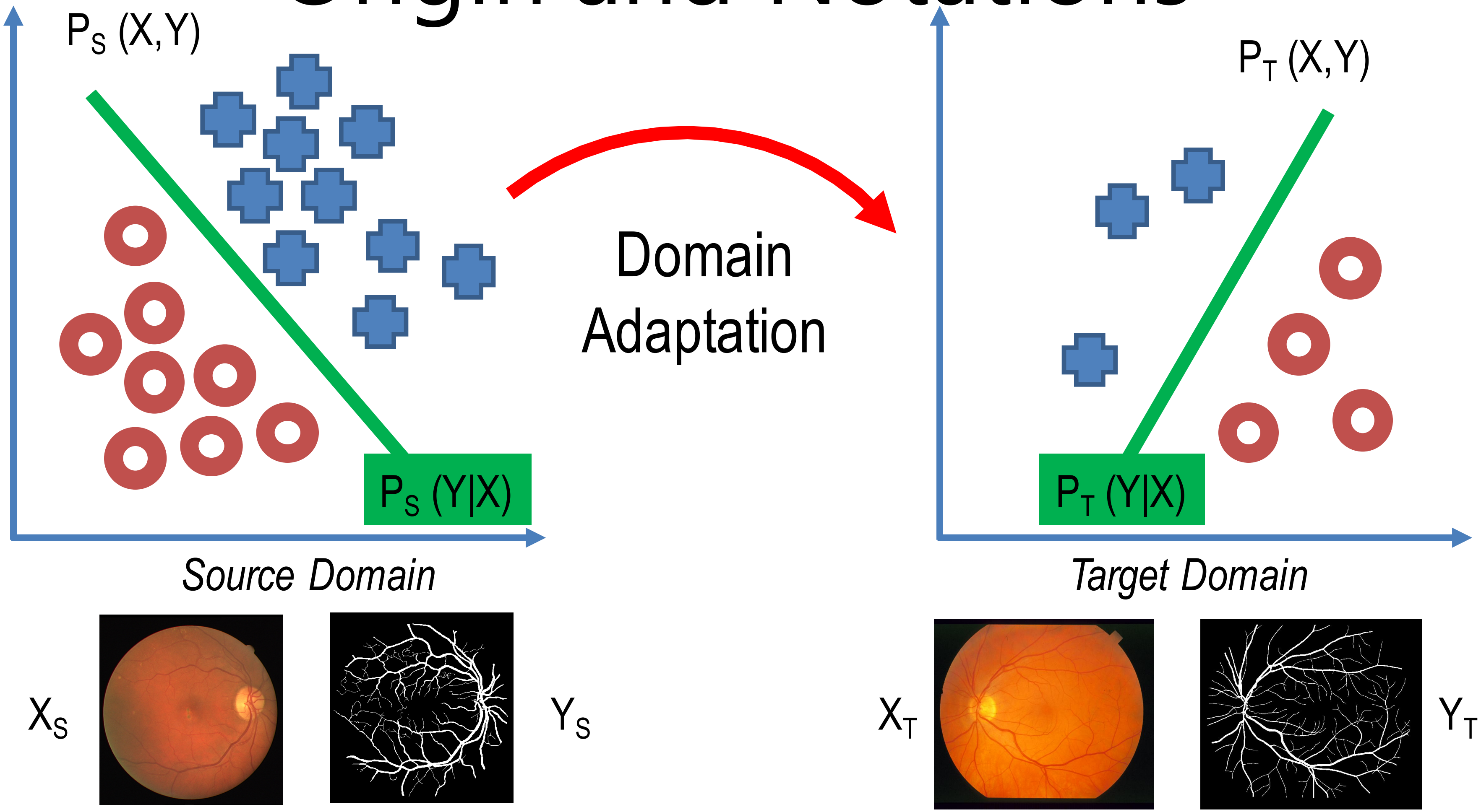

DA in Stacked Autoencoders

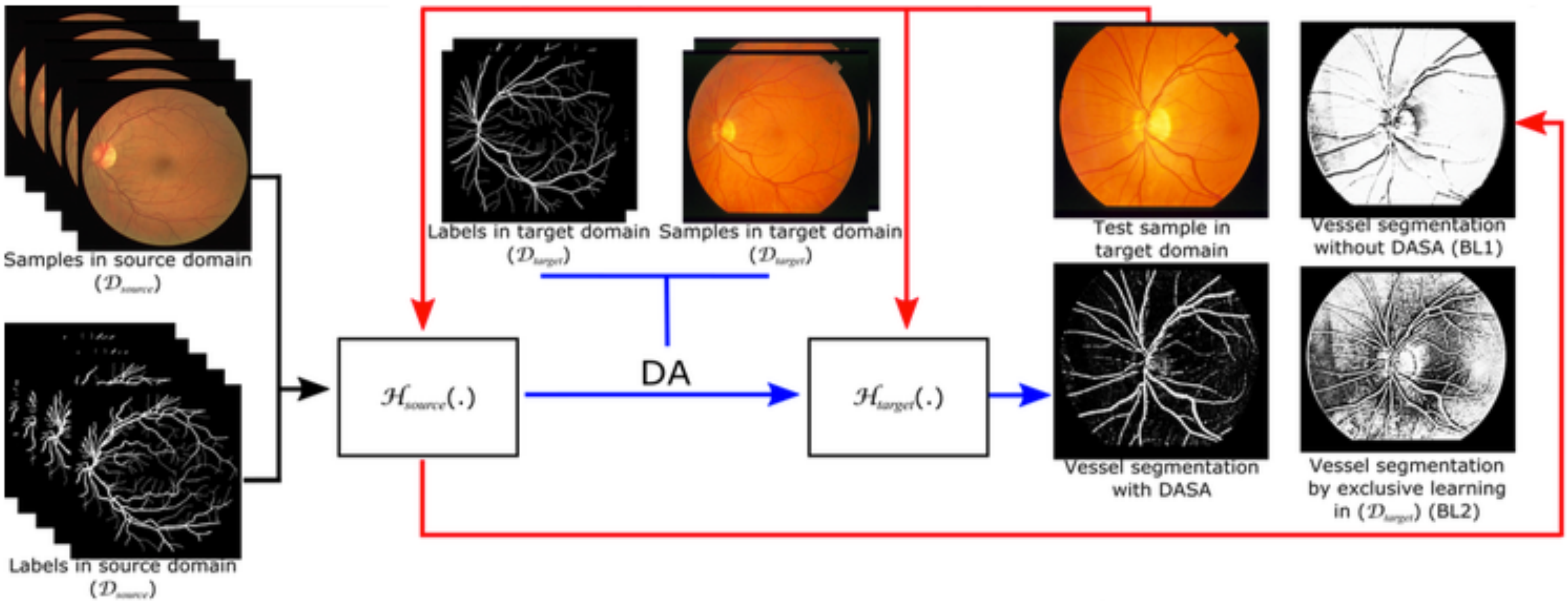

DA in Stacked Autoencoders (DASA) using Systematic Dropouts

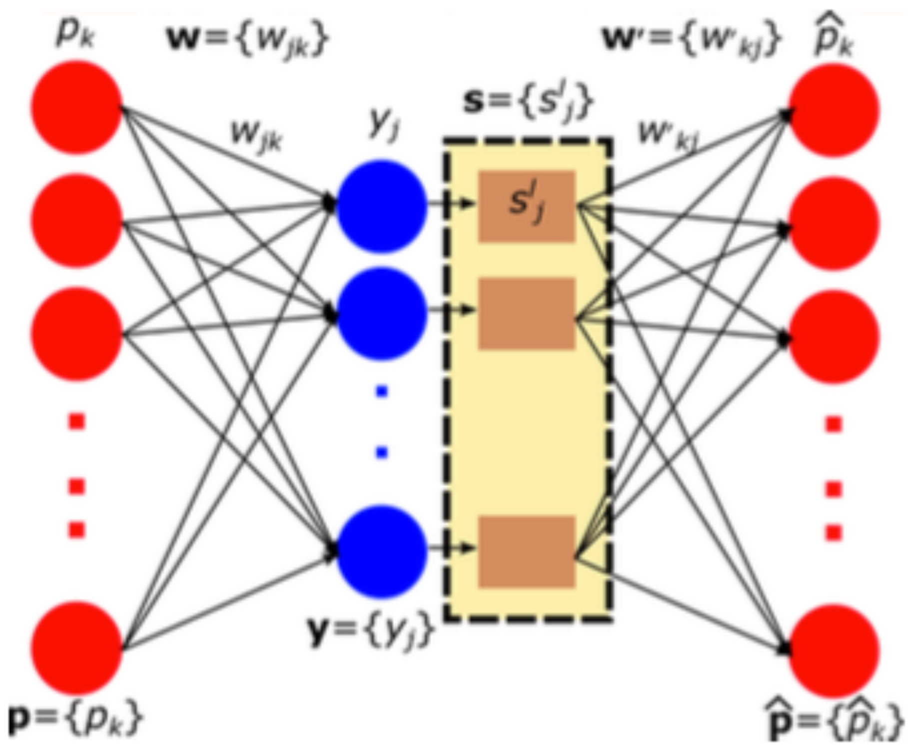

A. Guha Roy and D. Sheet, "Domain Adaptation in Stacked Autoencoders using Systematic Dropout", in *Proc. Asian Conf. Patt. Recognition*, 2015.

DASA: Performance and Learning

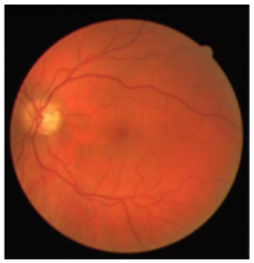

(a) Source domain sample.

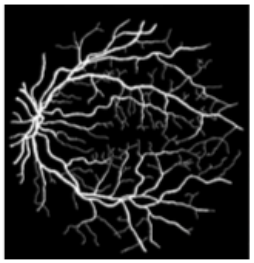

(b) Source domain labels.

(c) Source domain prediction.

(d) Target domain sample.

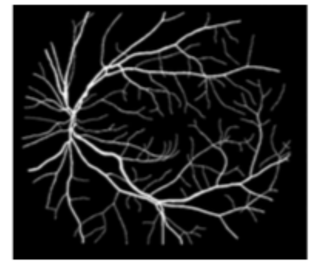

(e) Target domain labels.

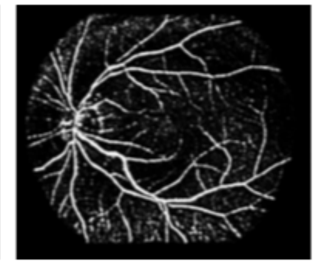

(f) Target domain prediction with DA.

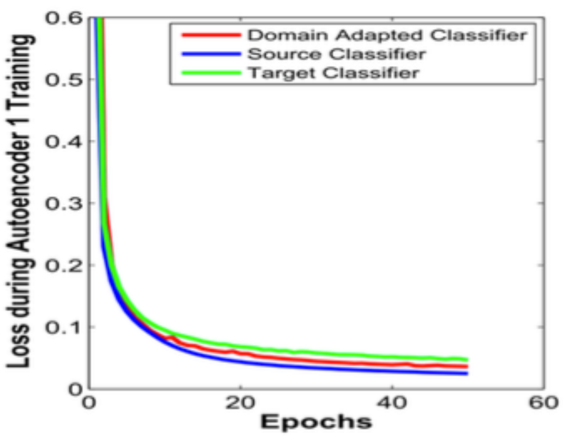

(k) $J(\mathbf{W})$ vs. epochs in training AE1

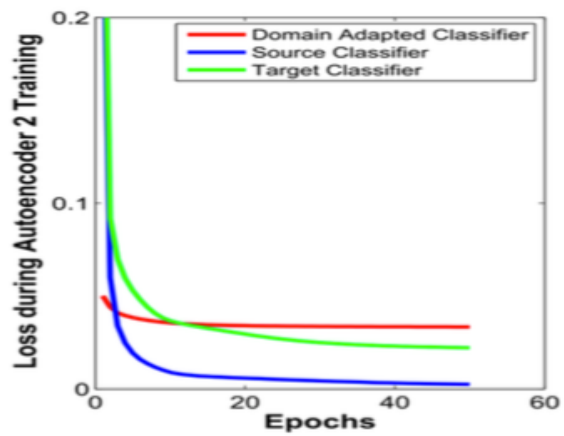

(l) $J(\mathbf{W})$ vs. epochs in training AE2

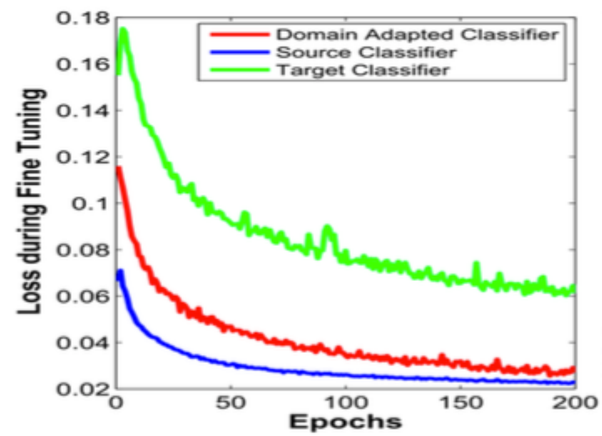

(m) $J(\mathbf{W})$ vs. epochs in training SAE-DNN

Take Home Messages

- Michael D. Abramoff, Mona K. Garvin, Milan Sonka, "Retinal Imaging and Image Analysis," IEEE Rev. Biomedical Engg., vol. 3, pp. 169 – 208.